Fabrication of Au/Si nanocomposite structure by nanosecond pulsed laser irradiation

Yutaka Yoshida[1], Seiichi Watanabe[1, 2], Yoshiaki Nishijima[3, 5], Kosei Ueno[3], Hiroaki Misawa[3], and Takahiko Kato[4]

[1] Division of Quantum Science and Engineering, Graduate School of Engineering, Hokkaido University, Kita-8, Nishi-13, Kita-ku, Sapporo, Hokkaido 060-8628, Japan

[2] Center for Advanced Research of Energy and Materials, Faculty of Engineering, Hokkaido University, Kita-8, Nishi-13, Kita, Sapporo, Hokkaido 060-8628, Japan

[3] Research Institute for Electronic Science, Hokkaido University, Sapporo, Hokkaido 001-0021, Japan

[4] Hitachi Research Laboratory, Hitachi, Ltd., 7-1-1 Omika, Hitachi, Ibaraki 319-1292, Japan

Present address: [5] Graduate School of Engineering, Yokohama National University, 79-5 Tokiwadai Hodogayaku, Yokohama, Japan

[*]**E-mail:** yyoshida@ufml.caret.hokudai.ac.jp **and** sw004@eng.hokudai. ac.jp

Abstract. A gold/silicon nanocomposite structure (NCS) was formed on a Si(100) surface by nanosecond pulse laser irradiation. The Au/Si NCS contained both Au nanoparticles (NPs) and Au-Si alloy layers. We report that the use of laser irradiation to form Au NPs comprises two competing processes: a top-down effect involving decomposition into smaller NPs and a bottom-up effect involving self-assembly or self-organization into larger NPs. The formation of the periodic structure involved self-organization, i.e., the bottom-up effect, and was observed *in situ* using a pulsed-laser-equipped high-voltage electron microscope. The NCS formed by laser irradiation can be controlled by adjusting the laser energy density and the number of laser pulses.

1. Introduction

Nanocomposite structures (NCSs) containing both metals and semiconductors are expected to have important practical applications due to the fact that they exhibit surface plasmon resonance (SPR). In particular, metal nanoparticles (NPs) and nanostructures assembled with dielectric matrices have attracted sustained interest owing to their unusual properties [1-10]. To date, metal/semiconductor NCSs used as electro-optical quantum device materials have been required to contain Au and Si, because metal-dielectric NCSs exhibit a fast optical response to SPR [8-10].

The optical properties of nanodevices are strongly influenced by the nanostructure size and

dimensions. Therefore, techniques for controlling the size and dimensions by employing top-down and bottom-up approaches have been widely discussed [10-20]. Nanotechnological approaches, such as melt quenching, the vapor-liquid-solid (VLS) method using metal dielectrics [10-15], metal-ion implantation of semiconductors [4, 5, 16], and pulsed laser irradiation [17, 18] have led to a transition in the size and dimensions of metal NPs and the nanostructure in NCSs. The present authors have also reported a novel top-down and bottom-up approach for fabrication of nanostructures such as Laser Induced Periodic Surface Structure (LIPSS)-dots on the surface of Si substrates using single-beam laser irradiation [19, 20].

In the present study, we demonstrate the fabrication of a Au/Si NCS by single-beam laser irradiation, which can be controlled by varying the laser energy density and the number of nanosecond pulses, and we present the internal structure of the Au/Si NCS, which was determined by structural analysis using an electron microscope.

2. Experimental Methods

Au NPs on Si surfaces were irradiated *ex situ* by pulsed laser radiation. A sample was prepared with a Au NP layer deposited on a silicon substrate using physical vapor deposition at room temperature in a vacuum chamber. The average thickness of the layer of granular Au NPs was 10 nm. The silicon substrate was n-type Si (100) (KN Platz Co., Ltd.) with a resistivity of 22 to 45 Ω·cm. After deposition, the Au/SiO_2/Si multilayer surface was irradiated in air at room temperature using a Nd:YAG pulse laser (Inlite II, Continuum Co., Ltd.) with a wavelength of 532 nm, a repetition frequency of 2 Hz, and a pulse width of 5 to 7 ns. The other laser conditions were as follows. The laser beam (beam diameter: 6 mm) was irradiated normal to the surface, and the average laser energy density was 1.24 kJ/m^2.

After laser irradiation, the surface morphology of the specimens was observed using a scanning electron microscope (SEM: JEOL JSM-6500), and microstructural and microchemical analyses were performed using a transmission electron microscope (TEM: JEOL JEM-2010F). In order to examine the distribution of the elemental concentration, elemental maps were acquired with a scanning transmission electron microscope (STEM: JEOL JEM-2010F EM-24015) and an energy-dispersive X-ray spectroscope (EDS: Noran Vantage). Microstructural observations and electron diffraction analyses were undertaken using the TEM and EDS, respectively. Two types of thin foil specimens were prepared for STEM and TEM observations using a focused ion beam (FIB).

In addition to the *ex situ* laser irradiation, we carried out an *in situ* observation of the formation process of Au NPs on the Si surface using a pulsed laser equipped with a high-voltage electron microscope (laser-HVEM). The laser source head of the Nd:YAG pulse laser used for the *ex situ* irradiation was mounted on the HVEM (H-1300, Hitachi, acceleration

voltage: 1,300 kV, point-to-point resolution: 0.204 nm) above the specimen, so that the linearly polarized laser beam could enter through a quartz window and irradiate the TEM specimen at an angle of 60°, which corresponds to a 30° (s-polarized) off-beam incidence condition. Prior to laser irradiation in the laser-HVEM, the laser beam passed through a 3-mm-diameter circular aperture immediately above the specimen such that the beam diameter was measured to be approximately 2 mm in terms of the full width at half maximum (FWHM) of its intensity profile. Since we did not use an optical focal lens in the present experiment, the laser energy density over the entire observation region of a TEM specimen with a typical diameter of several micrometers was presumed to be uniform. A video recording was taken during laser irradiation at a frame rate of 30 frames/s. Although the system was not sufficient for time resolution of the pulse duration, it was possible to monitor the microstructural evolution between successive pulses.

3. Results and Discussion

3.1 Top-down and bottom-up processes in the formation of Au/Si NCS by laser irradiation

Figure 1 shows SEM images of a Au/Si NCS surface observed after laser irradiation of (a) 0, (b) 50, (c) 500, and (d) 1,000 pulses at an average laser energy density of 1.24 kJ/m^2. After the irradiation of 50 pulses, however, spherical NPs were produced randomly on the surface, as shown in Figs. 1(c) and 1(d), dispersed NPs existed, and the size of the spherical NPs strongly depended on the number of laser pulses because the NPs after 500 and 1,000 pulses were much smaller than those after 50 pulses. Figure 1(e) shows the relation between the average NP diameter and the number of laser pulses, where the error bars indicate the maximum and minimum NP diameters for each number of pulses. It can be seen that the NP diameter decreased as the number of laser pulses increased. The TEM images inset in Fig. 1(e) also show the size of dispersed NPs on the surface, suggesting that their size can be controlled by varying the number of laser pulses. Moreover, the samples irradiated with 500 and 1,000 pulses have the possibility of an optical response near the SPR because the diameter of the produced NPs was less than 20 nm [21, 22].

On the other hand, as shown in Fig. 1(c) for the sample irradiated by 500 pulses, a periodic stripe structure formed by self-organization of NPs appeared on the Si surface [15, 16]. In Fig. 1(d), the larger dots correspond to a two-dimensional array layer, with variations in the X direction being due to the nanoscale periodic laser intensity distribution and those in the Y direction being due to the breakup of the stripe structure. The periodic structures formed by the top-down effect were perpendicular to the direction of laser polarization and had a periodicity of 530 nm in the X direction. The spacing Λ of stripes is obtained as follows:

$$\Lambda = \lambda / (1 \pm \sin\theta), \qquad (1)$$

where λ is the incident laser wavelength, and θ is the angle of incidence (the p-wave) of the laser beam [23]. The obtained results are in good agreement with Eq. (1) because the wavelength of the incident laser beam was 532 nm. Therefore, the periodic structure is considered to be formed, through a top-down effect, by the interference between the incident laser light and the scattered waves on the surface, as well as by conventional LIPSS [23-25]. The NCSs were found in the limited regions of laser-irradiation with high energy density. The area over which the periodic structure was observed was greater than 100 μm^2.

3.2 Bottom-up process in the formation of Au/Si NCS by laser irradiation

We carried out *in situ* observations to clarify the bottom-up process in detail. Figure 2 shows the formation of the periodic structure by the irradiation of multiple laser pulses at a lower energy density. The *in situ* laser-HVEM observation of random Au NPs on a TEM specimen surface revealed that both large and small Au NPs were initially randomly deposited on the surface and then moved with successive laser shots to form a periodic structure by agglomeration, thereby producing larger aligned dots.

The snapshot obtained after 120 pulses shown in Fig. 2(b) reveals that as the number of laser pulses increases, the NPs merged (see NPs 2 and 3 after 120 and 720 pulses in Figs. 2(b) and 2(c), respectively). A linearly ordered array of dots formed when some of the NPs underwent surface diffusion toward the same line, (e.g., NPs 1 through 7 move while changing their size and dimension in Figs. 2(c) and 2(d) after 720 and 1,320 pulses, respectively) and merged into larger dots (e.g., 2 into 3 and 6 into 7 after 1,560 and 1,830 pluses, respectively) forming a line of dots, as shown in Figs. 2(d) and 2(e). Such agglomerization of smaller NPs to form larger NPs is direct evidence of self-organization, as shown in Fig. 1(d). Moreover, larger aligned Au dots on Si thin film were also observed by *in situ* laser irradiation under the conditions described above, as shown in Fig. 2(h). These results reveal that the bottom-up process of moving (by surface diffusion) and merging of NPs on Si surface was due to the effects of laser irradiation and involved interference between the incident and scattered waves. These results indicate that the periodic structures were formed by both *in situ* and *ex situ* laser irradiation and consist of stripes and larger dots aligned in an ordered configuration.

3.3 Internal structure of the Au/Si NCS

In order to investigate the Au/Si NCS in detail, we carried out a cross-sectional TEM observation of the irradiated sample after 500 pulses. Figure 3 shows TEM and STEM images and EDS mappings after irradiation. Figure 3(a) shows a cross-sectional TEM image taken along the X direction in Fig. 1(c). The average distance between the stripes was 530 nm, and the average dimensions of the stripe structure were 244 nm in width, 12.5 nm in height, and

23.5 nm in depth from the surface. It is assumed that the optical property near the surface of Au/Si NCSs improves as the number of pulses increases owing to the periodic nanoscale surface roughness [26]. Figure 3(b) shows an enlarged high-angle annular dark-field scanning transmission (HAADF-STEM) image of the squared portion in Fig. 3(a). The interatomic diffusion between gold and silicon appears to have occurred upon laser irradiation because of the change in concentration with the location, as indicated by the contrast inside the stripe structure. Figures 3(c) through 3(f) show EDS mappings of the elemental distribution, which indicate that the NPs on the surface were made of gold, that the periodic stripe structure consisted primarily of a silicon and gold mixture, and that the interface between the NP layer and the periodic stripe structure consisted primarily of silicon and oxygen. Based on these results, we concluded that the NPs are Au NPs, that the interface region is a layer consisting primarily of silicon oxide, and that the periodic stripe structure is a Si-Au alloy. Therefore, the interdiffusion of Si and Au atoms was caused by the nanoscale temperature gradient resulting in the formation of Au-Si alloy at periodic locations. As shown in Figs. 3(g) and 3(h), we clarified the internal structure of a Au/Si NCS sample after irradiation.

3.4 High-resolution observation of the Au/Si NCS

Figure 4(a) shows an enlarged TEM image of the square portion in Fig. 3(a). The average diameter of the NPs was 8 nm, which is consistent with the diameter obtained by SEM observation. Figure 4(b) shows an HRTEM image of the center portion (red part) in Fig. 4(a), and the result of EDS analysis in this region is shown in Fig. 4(c). The Au NPs labeled l_1 in Fig. 4 were crystalline. Although the Au NPs were observed to be spherical on a few occasions, the spheres may have been droplets of molten gold [17]. A thin silicon oxide layer labeled l_2 (probably SiO_2) was found under the spherical Au NPs. Here, l_3 denotes a Si amorphous layer, whereas l_4 - l_6 denote multiple amorphous layers. Interdiffusion of Au and Si occurred, as indicated by the arrows labeled l_4 - l_6 [27]. It is considered that the silicon oxide layer remained thin due to the rapid heating during repeated pulsed laser irradiation with an interval of 5 to 7 ns followed by cooling, and the formation of the amorphous layer is attributed to rapid cooling. Although the Si (labeled l_7) remained crystalline, the laser heating had a thermal effect in regions in which elemental Au existed. The Au and Si peak intensities were approximately equal at l_3 and l_7 and at l_4 and l_6 and remained stable at these locations. In region l_8, complete Si crystallization occurred without Au diffusion.

According to the TEM image taken in the Y direction of the periodic structure in Fig. 1(c), the Au/Si alloy periodic structures embedded between the multilayers were also uniformly aligned in the cross section of the periodic structure, as shown in Fig. 4(d). Figure 4(e) shows an HRTEM image of the center portion (red part) in Fig. 4(d). The results of EDS analysis

performed at regions l_1 through l_8 in Fig. 4(b) are also consistent with the SEM, HAADF-STEM, and HRTEM observations. We concluded that the Au/Si alloy stripe structure was roughly uniformly shaped. It is considered that the internal structure of the periodic nanostructure can be established by diffusion control during the pulsed laser irradiation.

Although the details remain unclear, the mechanism of the competing top-down and bottom-up processes is concluded to be as follows. In the early stages, during the first 50 laser pulses, the laser beam light is mostly absorbed by the Au film. The Au NPs are first produced by ablation at the locally irradiated region and are redeposited as spherical Au NPs on the surface owing to surface tension. The spherical Au NPs remain randomly located under laser irradiation. The size of the NPs is then changed by the effects of subsequent laser pulses, which simultaneously induces a top-down effect, reducing their size due to ablation, and a bottom-up effect increasing their size due to re-agglomeration. These NPs then undergo aggregation into Au NPs under the thermal gradient on the surface, which is accompanied by bottom-up self-organization of stripes to form a periodic structure. The morphology then changes to form large periodic dots resulting from the breakup of the stripe structure [18]. This formation process of the periodic structure has been confirmed for a sample of dispersed Au NPs on a Si thin film (Fig. 2) as well as a Si thin film by *in situ* laser-HVEM measurement [19]. Moreover, Au-Si alloy agglomerates along the ripple line after surface diffusion. The layer of dispersed spherical Au NPs on the surface and the embedded Au-Si alloy layer between the silicon oxide and Si layers can be controlled by varying the laser energy density and the number of laser pulses.

4. Conclusion

We have investigated the formation of a Au/Si NCS with random spherical Au NPs on a silicon oxide layer with periodic Au/Si structures using single-beam laser irradiation which gives rise to competition between bottom-up and top-down processes. This is a simple approach without complex processes, and the sizes of spherical Au NPs and the periodic Au/Si structure can be simultaneously controlled by varying the number of laser pulses. Moreover, ordered aggregation of larger dots under laser irradiation has been directly clarified by the present *in situ* laser-HVEM study.

From the *ex situ* observation, the periodic Au/Si structure obtained after 500 pulses was a striped Au-Si alloy structure, which was embedded uniformly between a silicon oxide layer and bulk Si owing to the periodic interdiffusion by laser irradiation, resulting in the formation of a Au/Si NCS with uniformly-shaped stripe structures. It is suggested that the production of spherical Au NPs and the embedding of a periodic Au-Si alloy structure can be controlled by two competitive processes, a top-down effect and a bottom-up effect, using nanosecond pulsed

laser irradiation.

The freedom of selecting the type of Au/Si NCS using the simple laser irradiation approach proposed herein for the fabrication of metal/semiconductor NCSs on a surface has high potential for the development of quantum devices for quantum dot solar cell, quantum computer, and so forth.

Acknowledgments

The authors would like to thank Professors Shigeo Yatsu, Norihito Sakaguchi, Tamaki Shibayama, Norihiko Nishiguchi, and Heishitiro Takahashi for their helpful discussions and Dr. Yang Zhanbing and Mr. Kenji Ohkubo for their assistance with the operation of the laser-HVEM.

References

[1] Losurdo M, Giangregorio M M, Bianco G V, Sacchetti A, Capezzuto P, and Bruno G 2009 *Sol. Energy Mater. Sol. Cells*. **93** 1749-1754

[2] Pillaiv S, Catchpole K R, Trupke T, and Green M A 2007 *J. Appl. Phys*. **101** 93105-8

[3] Derkacs D, Lim S H, Mathen P, Mar W, and Yu E T 2006 *Appl. Phys. Lett*. **89** 093103

[4] Liao H, Wen W, and Wong G K L 2005 *J. Opt. Soc. Am. B* **23** 2518-4

[5] Dhara S, Kesavamoorthy R, Magudapathy P, Premila M, Panigrahi B K, Nair K G M, Wu C T, Chen K H, and Chen L C 2003 *Chem. Phys. Lett*. **370** 254-260

[6] Barnes W L, Dereux A, and Ebbesen T W 2003 *Nature* **424** 824-830

[7] Ozbay E 2006 *Science* **311** 189-193

[8] Hache F, Ricard D, and Flytzanis C 1986 *J. Opt. Soc. Am. B* **3** 1647-1655

[9] Haglund R F, Yang L, Magruder R H, Witting J E, Becker K, and Zuhr R A 1993 *Opt. Lett*. **18** 373-375

[10] Hu M-S, Chen H-L, Shen C-H, Hong L-S, Huang B-R, Chen K-H, and Chen L-C 2006 *Nat. Mater*. **5** 102-106

[11] Kwak D W, Cho H Y, and Yang W-C 2007 *Physica E* **37** 153-157

[12] Westwater J, Gosain D P, and Usui S 1997 *Jpn. J. Appl. Phys*. **36** 6204-6209

[13] Ressel B, Prince K C, and Heun S 2003 *J. Appl. Phys*. **93** 3886-3892

[14] Wakayama Y and Tanaka S 1997 *Nanostruct. Mater.* **8** 1033-1039

[15] Wakayama Y and Tanaka S 1999 *Nanostruct. Mater.* **12** 13-18

[16] Satpati B, Satyam P V, Som T, and Dev B N 2004 *Appl. Phys. A* **79** 447-451

[17] Trice J, Thomas D, Favazza C, Sureshkumar R, and Kalyanaraman R 2007 *Phys. Rev. B* **75** 235439-15

[18] Favazza C, Trice J, and Kalyanaraman R 2007 *Appl. Phys. Lett*. **91** 043105

[19] Watanabe S, Yoshida Y, Kayashima S, Yatsu S, Kawai M, and Kato T 2010 *J. Appl. Phys*. **108** 103510-5

[20] Yoshida Y, Yatsu S, Watanabe S, Kawai M, and Kato T 2010 *Jpn. Inst. Electron Packag*. **3** 57-61; Yoshida Y, Sakaguchi N, Watanabe S, and Kato T 2011 *Appl. Phys. Express* **4** 055202-3

[21] Kelly K L, Coronado E, Zhao L L, and Schatz G C 2003 *J. Phys. Chem. B* **107** 668-677

[22] Manzhou Z, Christine M A, Frederick J H, George C S, and Rongchao J 2008 *J. Am. Chem. Soc*. **130** 5883-5885

[23] Birnbaum M 1965 *J. Appl. Phys*. **36** 3688

[24] Young J F, Preston J S, Vandriel H M, and Sipe J E 1983 *Phys. Rev. B* **27** 1155-1172

[25] Sipe J E, Young J F, Preston J S, and Vandriel H M 1983 *Phys. Rev. B* **27** 1141-1154

[26] Qiu T, Wu L, Siu G G and Chu P K 2005 *Appl. Phys. Lett*. **87** 223115

[27] Chang J F, Young T F, Yang Y L, Ueng H Y, and Chang T C 2004 *Mater. Chem. Phys.* **83** 199-203

Figure captions

Figure 1. SEM images of Au/Si NCS on a surface irradiated at a repetition rate of 2 Hz and a laser energy density of 1.24 kJ/m^2 after (a) 0, (b) 50, (c) 500, and (d) 1,000 pulses. *E* indicates the electric field vector of the laser light on the surface under laser irradiation. (e) Average NP diameter versus number of laser pulses. The error bars indicate the maximum and minimum particle diameters. The insets are cross-sectional TEM images taken from samples irradiated by 50 and 1,000 pulses, indicating the formation of spherical NPs.

Figure 2. *In situ* laser irradiation and observation using laser-HVEM (1.2×10^{-5} Pa) of formation and self-organization of ordered periodic structure (larger dots) on a thin TEM silicon specimen during multiple pulses of laser irradiation at a repetition rate of 2 Hz and an average laser energy density of 0.27 kJ/m^2. (a)-(f) Snapshots of Au NPs and development of periodic structure on the surface after various numbers of pulses of laser irradiation recorded using laser-HVEM. (a) Start of recording, (b) 120, (c) 720, (d) 1,320, (e) 1,560, and (f) 1,830 pulses. (g) Schematic diagram of the plane-view configuration for *in situ* observation using laser-HVEM. (h) Snapshot of larger aligned dots on the thin Si surface after pulsed laser irradiation.

Figure 3. TEM and STEM images, EDS mappings, and cross-sectional illustrations of structure of Au/Si NCS after 500 pulses at an energy density of 1.24 kJ/m^2 in air. **(**a) Cross sectional image of X in the direction shown in Fig. 1(c). (b) HAADF-STEM image of the square portion labeled (b) in (a). (c)-(f) EDS mappings of silicon, gold, oxygen, and carbon, respectively, from one of the periodic structures in the square labeled (b) in (a). The outside part was a deposited carbon layer, as shown in (f), which was deposited when the cross-sectional specimens used for STEM and TEM were prepared using an FIB. (g) Before irradiation and (h) after irradiation.

Figure 4. TEM image and EDS point analysis of Au/Si NCS on the irradiated surface. (a) TEM image taken from square portion (b) in Fig. 3(a). (b) HRTEM image of center part labeled (*b*) in (a). (c) EDS point analysis: l_1 - l_8 in (c) correspond to l_1 - l_8 in (b). The outside part has a high carbon and copper concentration, as shown in (c), because of the C-DEPO layer grown using an FIB and the Cu grid used for the TEM sample. (d) TEM image in the Y direction in Fig. 1(c). (e) HRTEM image of the center part labeled (*e*) in (d).

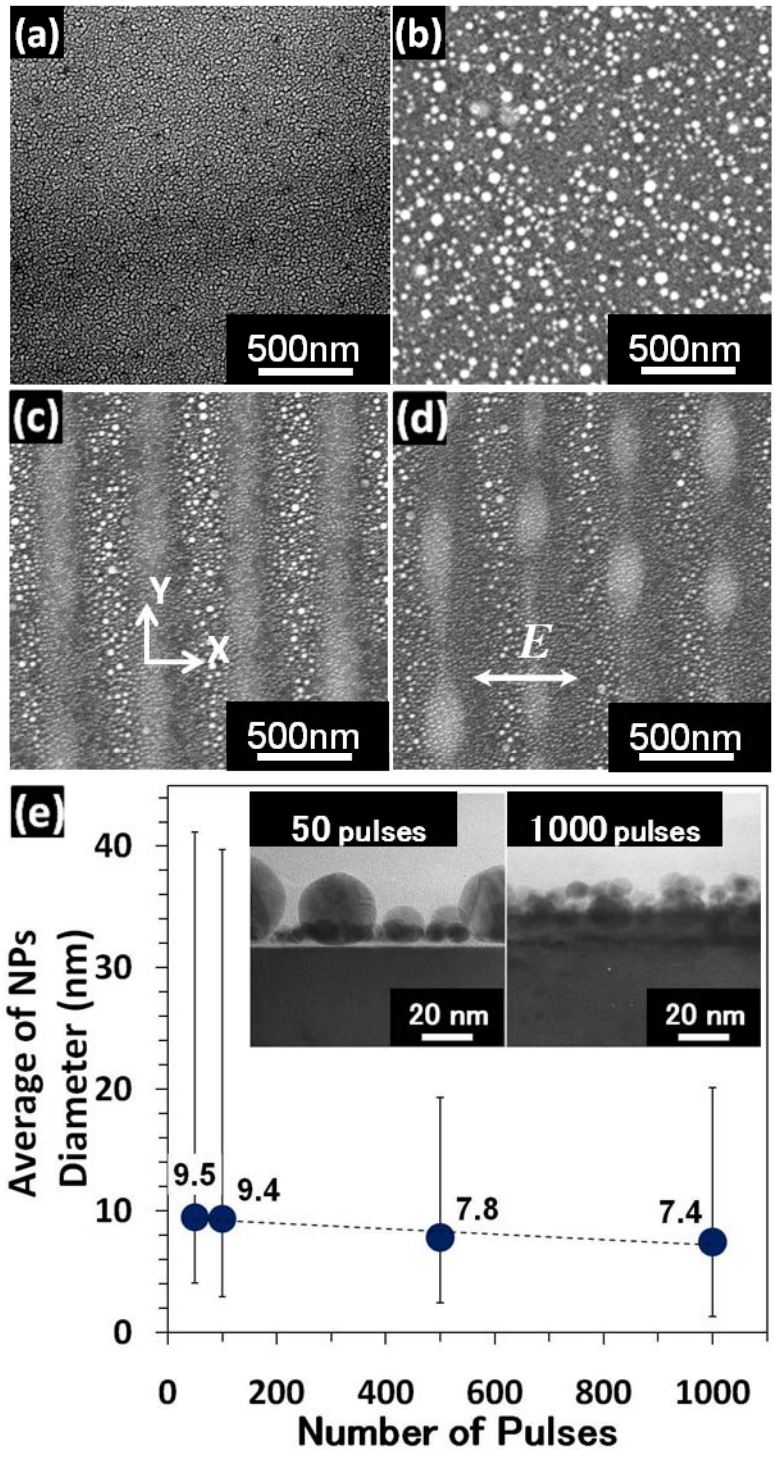

Figure 1. Yoshida

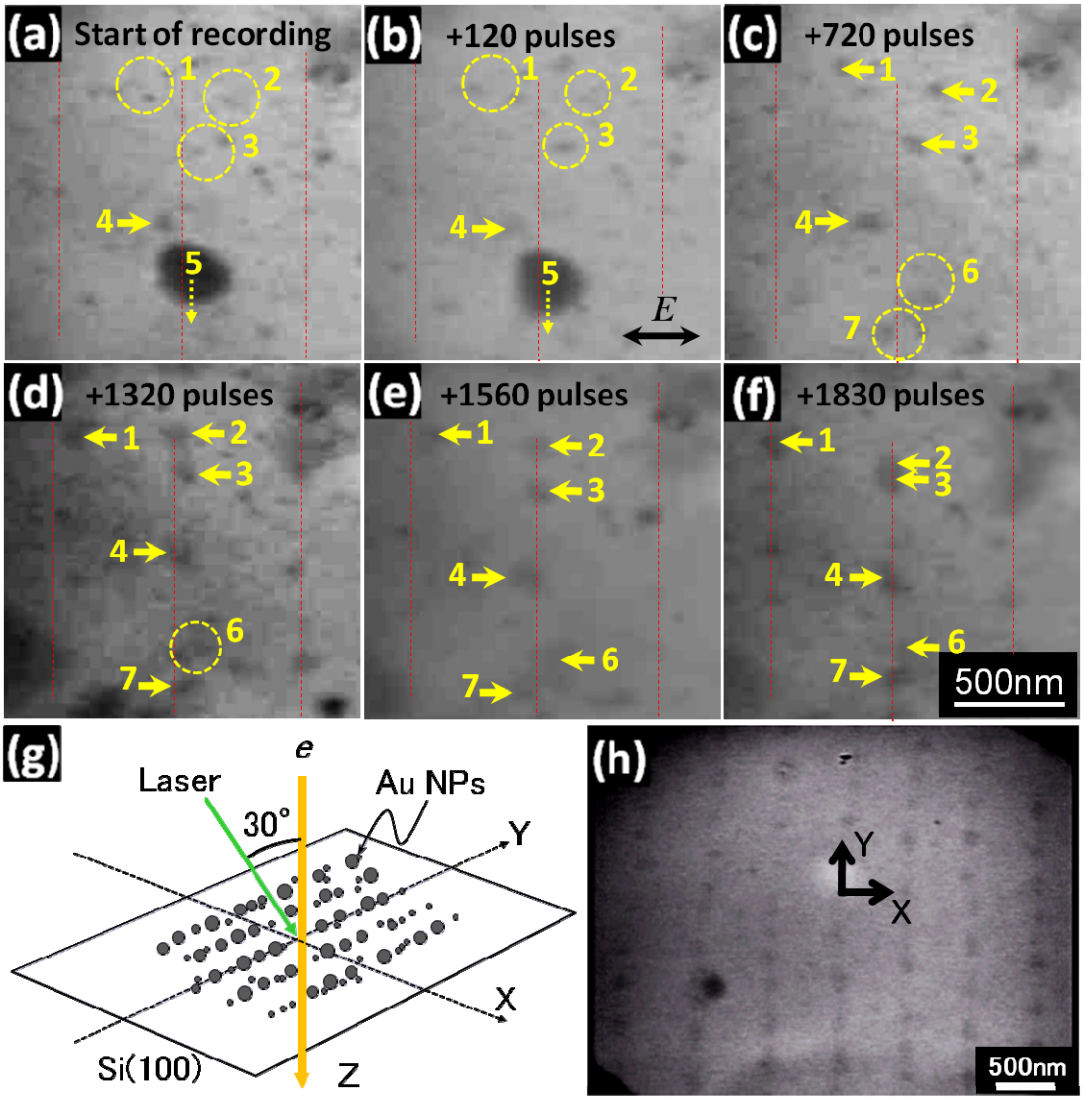

Figure 2. Yoshida

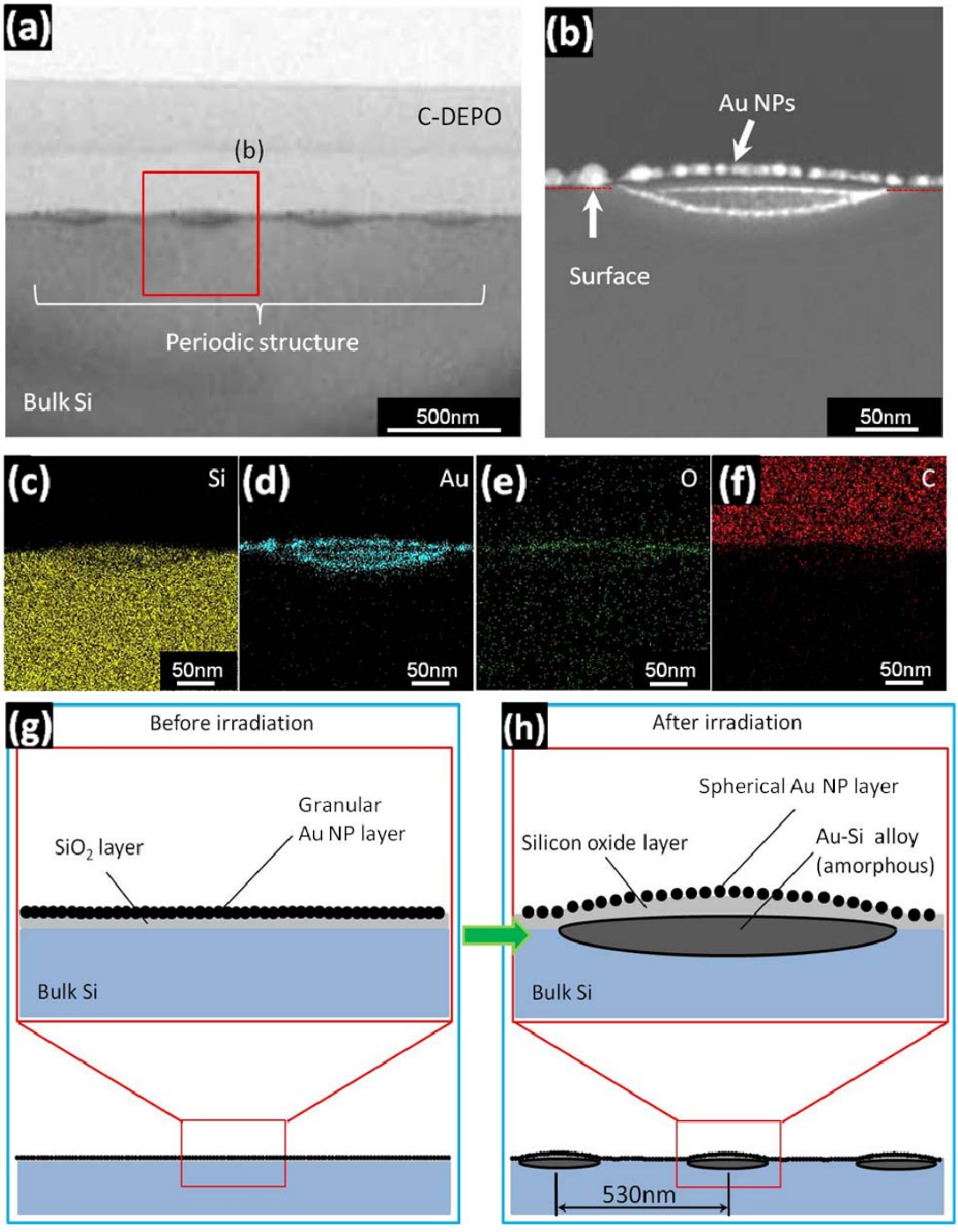

Figure 3. Yoshida

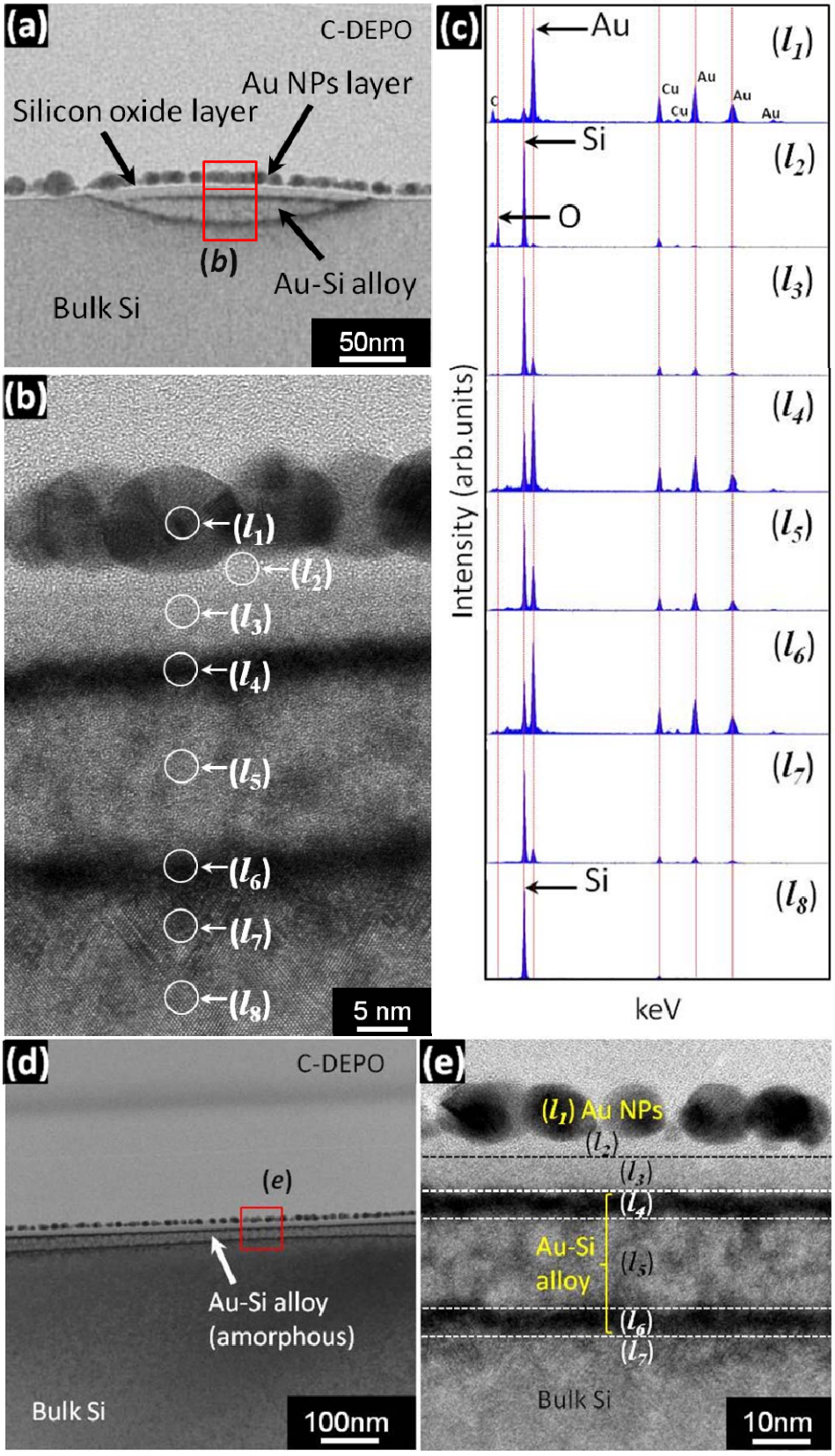

Figure 4. Yoshida